Is the H_0 measurement from Cepheids robust?

Matt Paterson, Supervisor: George Efstathiou

(Dated: 5 May 2020)

There is a 4.4σ inconsistency in the value of H_0 calculated by the traditional distance ladder method (Reiss et al 2019) and the value inferred from cosmic microwave background (CMB) anisotropies (Planck Collaboration 2018). We test the consistency of two principal distance anchors used in Reiss's work using Cepheids from (Reiss et al 2016, 2019). We conclude a 3.5σ discrepancy in geometric distance moduli and a 4.3σ discrepancy in Cepheid P-L relation slopes using χ^2 minimization fits, suggesting the possibility of systematic bias in Reiss photometry. We use two independent geometric distance estimates: 20 detached eclipsing binaries in the LMC and a water masing accretion disc in NGC 4258 to calibrate the Cepheid distance scale. Using the distance anchors we directly calculate the peak luminosities of SNe Ia in Cepheid host galaxies, and use these to calculate H_0.

1 INTRODUCTION

In 1929 Edwin Hubble discovered the expansion of the universe, first estimating H_0 to be approximately 550 km s^{-1} Mpc^{-1}. If the universe had expanded at a constant rate in the past, this would imply the age of the universe now to be the inverse, 1.8 billion years. It was believed by geologists in the 1920s that the Earth was probably over 2 billion years old, in disagreement with Hubble's value. This motivated analysis of Hubble's work and also the development of radically different cosmologies such as the steady state theory. In the 1950s, significant errors were discovered in Hubble's distance scale. Since then, H_0 has remained difficult to measure.

However, considerable progress has been made, assisted by observations of water masers, strong-lensing systems, SNe, the Cepheid Period-Luminosity (P–L) relation and other sources used to construct distance ladders, most recently by the SH0ES (SNe, H_0, for the Equation of State of dark energy) team.

Using independent geometric distance estimates to distance anchors, the distance ladder method calibrates the Cepheid P-L relation from Cepheids in nearby anchors. With this scale calibrated we can calculate the absolute magnitude for recorded 1a SNe in host galaxies that contain Cepheids, then using the Supernovae magnitude-redshift relation, determine H_0.

Recent work (Reiss et al 2009, 2011, 2016, 2019, hereafter R9 R11 R16 R19) gives a distance ladder best estimate of:

$$H_0 = 74.03 \pm 1.42 \text{ km s}^{-1} \text{ Mpc}^{-1}. \quad (1)$$

This estimate uses four geometric distance calibrations of Cepheids: water maser disc geometry in NGC 4258, 20 detached eclipsing binaries (DEBs) in the LMC, parallax measurements of Cepheids in the Milky Way and DEBs in M31.

1.1 PLANCK INCONSISTENCY

Independent calculation of H_0 is also possible via observations of the CMB in accordance with current ΛCDM cosmology. This gives (Planck Collaboration 2018):

$$H_0 = 67.4 \pm 0.5 \text{ km s}^{-1} \text{ Mpc}^{-1}. \quad (2)$$

There is a 4.4σ disagreement with the traditional distance ladder best estimate (1).

Some arguments suggest that this discrepancy requires modification to the early universe model, others that the Cepheid data are affected in some way by systematic error. It has proved difficult to provide early universe solutions to this problem, although some models have been proposed. See (Knox and Millea 2019) for a review. The possibility of discovering new physics has provided strong motivation to subject both the CMB and distance ladder methods to intense scrutiny.

1.2 PROJECT AIM

A Cepheid variable star is a star that radially pulsates due to the Eddington valve/ κ- mechanism. The varying temperature and diameter during oscillation gives a useful P-L relation, allowing determination of luminosity and hence distance via observation of period.

The aim of this project is to test the consistency of the principal distance anchors using R16 Cepheids. Inconsistencies may suggest problems with Riess's photometry. We will look specifically at the LMC and NGC 4258 distance anchors. Comparing the P-L slopes will give another test of photometry consistency.

2 METHOD

The foundation of the work to determine H_0 in the distance ladder method is to construct the Cepheid P-L relation. The data used contains appropriate measurements for thousands of Cepheids from different systems with varying metallicities to calculate this. Table 1 is a summary to indicate the type of data we use, from the distance anchor galaxy NGC 4258.

The measurements required are period P (days), $V-I$ colour (mag), H-Band magnitude m_H (mag), magnitude error e (mag) and metallicity $\log_{10}(O/H)$. The magnitude errors can be large because of crowded fields around the Cepheids. We must also account for wavelength dependent extinction caused by the interstellar medium and dust in the host galaxy by calculating "Wesenheit" magnitudes. This is possible by measuring magnitudes in

period	$V-I$	m_H	σ	metallicity
14.81	1.20	22.80	0.226	8.787
19.96	1.40	22.38	0.266	8.826
60.98	1.53	21.62	0.169	8.786
26.83	1.32	23.12	0.230	8.863
30.90	1.33	22.61	0.179	8.867
57.49	1.36	21.18	0.203	8.883
16.86	1.35	22.78	0.271	8.804
31.19	1.27	22.46	0.182	8.776
21.26	1.38	22.50	0.192	8.772
6.16	1.08	24.79	0.428	8.749

TABLE I: The first 10 Cepheids from R16 Hubble Space Telescope data on NGC 4258 Cepheids.

different bands, (H, V, I) and defining our corrected magnitudes as:

$$m_H^W = m_H - 0.386(V-I). \tag{3}$$

This reduces the scatter in the P-L relation. The value of 0.386 is for a Galactic extinction law. There is a subtle issue here because the LMC has lower metallicity than the SN host galaxies and some speculate that the dust extinction law may be different to that of large galaxies. Refer to R16 for a detailed discussion on how altering the Wesenheit law affects calculation of H_0. Hereafter all instances of magnitude m will be Wesenheit magnitude as defined in (3).

2.1 χ^2 MINIMISATION

To determine the P-L relation, all Reiss papers use a χ^2 minimisation method. I have replicated certain parts of this work in my project using the same technique, for appropriate comparison. Linear algebra is used to express the proposed models, along with a symmetric correlation matrix containing the uncertainties. We invert the matrices to derive the maximum-likelihood parameters for our proposed model. So for a linear model estimating m with dependent variables d_i:

$$m(d_1, d_2, d_3, ...) = \sum_i c_i d_i, \tag{4}$$

we have measurements for each Cepheid:

$$(m_j, d_1^j, d_2^j, d_3^j, ...), \tag{5}$$

and an overall χ^2:

$$\chi^2 = \sum_j \frac{(m_j - \sum_i c_i d_i^j)^2}{\sigma_j^2}. \tag{6}$$

To minimise this, hence maximise the likelihood function giving us best fit parameters, we vary:

$$\frac{\partial \chi^2}{\partial c_i} = 0 \ , \ \forall i, \tag{7}$$

which after calculation gives us a set of simultaneous equations rearranged into a linear system with Fisher matrix F:

$$\sum_j F_{ij} c_j = \sum_j m_j d_i^j, \tag{8}$$

where the correlation/Fisher matrix is expressed as:

$$F_{ij} = \frac{\partial^2 \chi^2}{\partial c_i \partial c_j}. \tag{9}$$

The system is then simply inverted to solve for our best fit parameters:

$$(c_1, c_2, c_3, ...). \tag{10}$$

Diagonal elements of the inverted Fisher matrix F_{ij}^{-1} provide accurate estimation of parameter error, so the square route of this we calculate as the error term. Hence results for fitted parameter c_i are displayed as:

$$c_i \pm \sqrt{(F_{ii}^{-1})}. \tag{11}$$

2.2 ADDING PRIORS

At certain points we wish to enforce a prior on the models, reflecting a belief on a certain parameter d_k to be close to d_k^0 before the fit is run. This can be done by adding the term:

$$\frac{(d_k - d_k^0)^2}{\sigma_{d_k}^2} \tag{12}$$

to the χ^2, where σ_{d_k} is manually input to reflect our level of conviction.

3 LMC R19

To obtain an accurate estimate of the Cepheid P-L relation we want to examine the most precise Cepheid measurements. First we look at R19 measurements of 70 Cepheids in the Large Magellanic Cloud (LMC), LMC is our nearest Cepheid-rich neighbour galaxy. This photometry is done on the HST Wide Field Camera 3 (WFC3) to give very precise results, which is also the same photometry system used for the SN host galaxies, removing the possibility for cross-instrument zero-point errors.

With a gemoetric distance estimate to LMC, we can directly calculate the absolute magnitudes of the Cepheids. The LMC geometric distance modulus is determined from observations of 20 detached eclipsing binary (DEB) stars (Pietrzynski et al 19, P19). These DEB measurements appear quite robust, all 20 DEBs are consistent, yielding a distance modulus of:

$$\mu_{LMC} = 18.477 \pm 0.026 \text{ mag}. \tag{13}$$

We now fit the Cepheids j to the relation:

$$m_j = \mu_{LMC} + c + b(\log_{10} P_j - 1) + Z\Delta \log_{10}(O/H)_j, \quad (14)$$

where the difference from solar metallicity is defined as:

$$\Delta \log_{10}(O/H) = \log_{10}(O/H) - 8.9. \quad (15)$$

Parameter c represents the fitted absolute magnitude of an LMC cepheid with a period of 10 days, b the slope of the P-L relation and Z the metallicity dependence. To run the fit we impose a tight prior on the metallicity dependence Z forcing it to be 0. The range of metallicities in a single system is small and causes statistically insignificant results, particularly in the LMC where all cepheids are listed to have a metallicity of 8.650.

Before fitting we add an intrinsic scatter term σ^{int}, as Reiss does, to the total magnitude error term for each Cepheid in quadrature:

$$(\sigma_j^{tot})^2 = (\sigma_j)^2 + (\sigma^{int})^2. \quad (16)$$

This is to account for the extra variation caused by the non-zero temperature width of the Cepheid instability strip on the HR diagram. Reiss determines $\sigma^{int} = 0.08$ in R16 by forcing a χ^2 per degree of freedom of unity. I use the same value.

Because of the inclination of the LMC, we also expect some Cepheids to be closer or farther than average by a few hundredths of a magnitude in distance modulus. This has been detailed and corrected for in the data used from R19 and P19, a small correction with average 0.001 mag.

This gives us χ^2 summing over individual Cepheids j of:

$$\chi^2 = \sum_j \frac{(m_j - \mu_{LMC} - b(\log_{10} P_j - 1) - c)^2}{(\sigma_j^{tot})^2}. \quad (17)$$

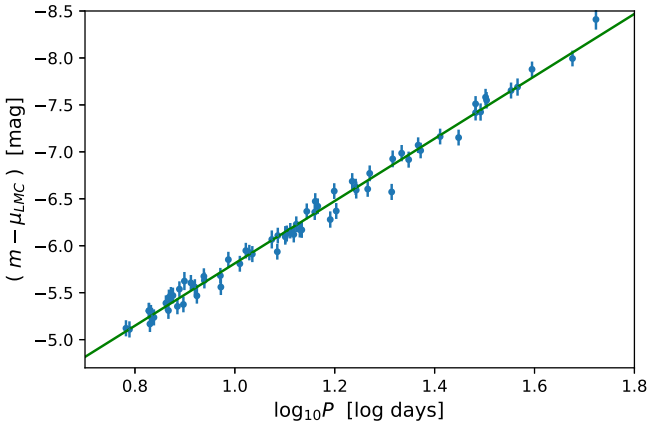

FIG. 1: The P-L relation of LMC Cepheids including error bars. Absolute magnitude plotted against $\log_{10} P$ and fitted model (17) included.

After minimising and solving we find:

$$\begin{aligned} &LMC && b = -3.321 \pm 0.043, \\ &\text{All Periods} && c = -5.812 \pm 0.012. \end{aligned} \quad (17)$$

We note the reasonably low errors, although we don't have many data points for this sample, the LMC P-L relation is well defined because the photometry is so accurate and LMC is close to us. Figure 1 shows a plot of this fit.

4 NGC 4258

Now that we have a base to compare our P-L relations with, we want to look at other systems. We investigate another distance anchor, the spiral galaxy NGC 4258 (also known as Messier 106). The observations of NGC 4258 uses the same photometric system as the LMC data so we can compare the two without photometry difference. We use data for 139 Cepheids from R16.

NGC 4258 also has a well-defined geometric distance modulus which can be used as a distance anchor. It is used as an anchor extensively throughout the Reiss papers, as it has Cepheids with a similar metallicity to those found in the SN host galaxies used in the global fit to determine H_0. Observations of megamasers in Keplerian motion around a supermassive blackhole in NGC 4258 (Reid et al. 2019) give:

$$\mu_{N4258} = 29.397 \pm 0.033 \text{ mag}. \quad (18)$$

We model the system as in (14):

$$m_j = \mu_{N4258} + c + b(\log_{10} P_j - 1) + Z\Delta \log_{10}(O/H)_j, \quad (19)$$

with associated χ^2:

$$\chi^2 = \sum_j \frac{(m_j - \mu_{N4258} - b(\log_{10} P_j - 1) - c)^2}{(\sigma_j)^2}. \quad (20)$$

Using 139 Cepheids in NGC 4258 from R16 we run the fit, again forcing $Z = 0$ due to the small metallicity range spanned to give:

$$\begin{aligned} &NGC\ 4258 && b = -3.144 \pm 0.098, \\ &\text{All Periods} && c = -6.039 \pm 0.040. \end{aligned} \quad (21)$$

As it is further away than the LMC, we can see that the relation is not as well defined, the errors are significantly larger. Note in figure 2 that the brighter the Cepheid the smaller the error. There is a slope discrepancy between the b value for the previous LMC fit, of 1.7σ, not largely significant but we will investigate this later using the full SN host galaxy sample. Importantly this slope discrepancy is independent of the values we have chosen for distance moduli.

5 JOINT FIT

We can test the consistency of the geometric distance moduli by using Cepheids in both galaxies. We use a joint fit, fixing the LMC geometric distance modulus μ_{LMC} (13) whilst varying for slope b, intercept c and NGC 4258 distance modulus μ_{4258}^p to:

$$m_j^{LMC} = \mu_{LMC} + c + b(\log_{10} P_j - 1), \quad (22)$$

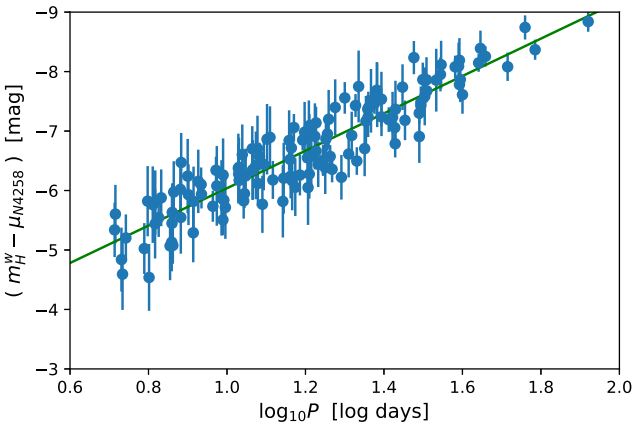

FIG. 2: The Period Luminosity relation of NGC4258 Cepheids including error bars. Absolute magnitude plotted against $\log_{10} P$ and (21) fit included.

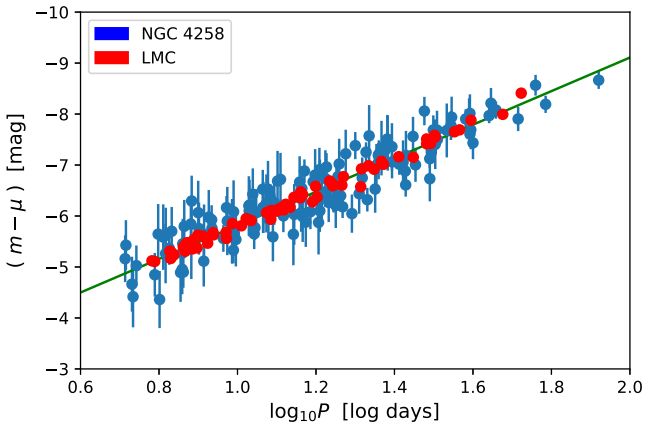

FIG. 3: The Period Luminosity relation of LMC and NGC 4258 Cepheids from running a joint fit on R19 and R16 data. Absolute magnitude calculated with μ_{LMC} and μ^P_{NGC} plotted against $\log_{10} P$ and (24) fit.

$$m_j^{NGC} = \mu^P_{NGC} + c + b(\log_{10} P_j - 1), \tag{23}$$

again forcing a strict 0 prior on the metallicity dependence. If we added a metallicity dependence it would become degenerate with distance modulus. This fit (shown in figure 3) gives:

$$\begin{aligned} \text{All Periods} \qquad b &= -3.292 \pm 0.039, \\ c &= -5.816 \pm 0.011, \\ \mu^P_{NGC} &= 29.221 \pm 0.029. \end{aligned} \tag{24}$$

We see the fitted modulus differs to (18), so adding the errors of μ_{LMC}, μ_{NGC}, and μ^P_{NGC} in quadrature we calculate:

$$\Delta\mu = \mu_{4258} - \mu = 0.177 \pm 0.051. \tag{25}$$

A discrepancy of almost 3.5σ exists. This places NGC 4258 at distance of 6.89Mpc instead of the maser distance 7.58Mpc. For a metallicity dependence to explain this difference, using means $\langle \log_{10}(O/H)\rangle_{NGC4258} = 8.90$ and $\langle \log_{10}(O/H)\rangle_{LMC} = 8.65$, a quick calculation indicates a required $Z = -1.40$. This is several times larger than indications in global fits of R16 give and so implausible.

There must be an inconsistency in one of: the LMC geometric distance (13); the NGC4258 geometric distance (18); the established Cepheid P-L analysis. This is important because all three are used in Reiss's 'best estimate' calculation of H_0. Investigating either distance measurement is outside the scope of this project, so instead we look at possibilities for errors in the calculation of the Cepheid P-L relation.

6 LMC GROUND PHOTOMETRY

Having seen slope and distance discrepancies we want to investigate how we can further constrain the P-L relation, particularly to investigate the possibility of a break in the relation's linearity. We require more data points. The LMC is close to us and has been imaged extensively from the ground, not possible for NGC 4258 due to its distance. R16 uses such a set of 775 LMC Cepheids obtained with ground-based photometry. We compare this to the R19 photometry. There are 67 mutual Cepheids in common between the ground and the HST photometry. To investigate if there is a significant offset we fit a linear relation between the two sets of magnitudes and minimise χ^2, accounting for errors in both samples by adding the individual errors in quadrature. Fitting to the linear model:

$$m_j^H = p(m_j^G) + q, \tag{26}$$

with χ^2:

$$\chi^2 = \sum_j \frac{(m_j^H - p(m_j^G) - q)^2}{\sigma_H^2 + \sigma_G^2}, \tag{26}$$

we find:

$$\begin{aligned} p &= 1.010 \pm 0.015, \\ q &= -0.064 \pm 0.187. \end{aligned} \tag{27}$$

The slope is consistent with unity. Forcing the slope to be unity gives:

$$q = 0.063 \pm 0.011. \tag{28}$$

See figure 4. We apply this offset to the 775 LMC ground Cepheids to bring them in accordance with the HST photometry. Now using a single fit on the modified 775 Cepheids with the same models as (14) we find:

$$\begin{aligned} LMC \qquad b &= -3.256 \pm 0.012, \\ \text{All Periods} \quad c &= -5.843 \pm 0.005. \end{aligned} \tag{29}$$

The fit is shown in figure 5. The LMC P-L slope is now tightly constrained and we can use the modified set of ground data to investigate linearity.

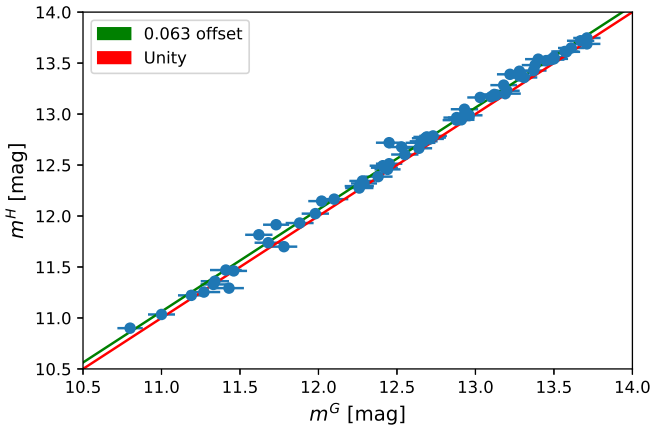

FIG. 4: Comparison of 67 Cepheid measurements from R19 HST and R16 ground-based photometry , plotted against line of unity and best fit offset line.

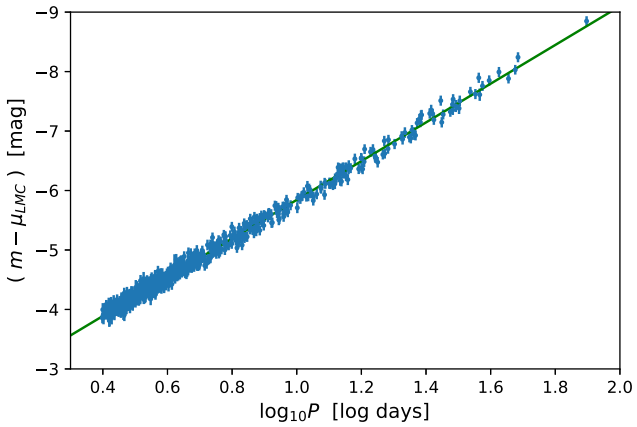

FIG. 5: Single fit to 775 LMC cepheids from ground-based photometry after correcting for (28) offset

7 NON-LINEARITY

There are some claims for departures from a pure power law P-L relation for $P > 60$ days (Persson et al., 2004; Freedman et al. 2012; Scowcroft et al. 2011) and $P > 10$ days (Ngeow et al. 2005). Due to LMCs close proximity, the ground photometry sample contains many Cepheids below and above the ten day period mark. There are few $P < 10$ days Cepheids in SN host galaxies and NGC 4258 due to their increased distance. Shorter period Cepheids are fainter and so harder to measure at larger distances.

To explore non-linearity, we can run single fits for restricted period samples of the LMC ground data. For the period ranges stated below we find slope results:

$$\begin{aligned} P > 40 \text{ days} \quad & b = -3.509 \pm 0.349, \\ P > 30 \text{ days} \quad & b = -3.467 \pm 0.201, \\ P > 20 \text{ days} \quad & b = -3.412 \pm 0.123, \\ P > 10 \text{ days} \quad & b = -3.390 \pm 0.060, \\ P < 10 \text{ days} \quad & b = -3.221 \pm 0.031. \end{aligned} \tag{30}$$

There aren't enough high period Cepheids to conclude about a break at $P = 60$ days but we can see that there is a significant 2.5σ break between $P > 10$ days and $P < 10$ days slopes. We will exclude Cepheids with $P < 10$ days for the global fits to avoid a possibility for error caused by this break.

8 R11 VS R16 NGC 4258

Returning attention to the distance anchor NGC 4258, the R16 data set we used in section 4 comes from a similar set used in R11. Both analyses use the same H-band HST images. R16 redid the photometry and imposed colour cuts to reduce the number of outliers. We want to compare the R11 and R16 photometry, Cepheid by Cepheid, to understand the differences.

Individual Cepheids are not resolved in SN host galaxies, even with the high resolution of the HST. As a consequence all of the Cepheids are contaminated by nearby stars and must be deblended to high accuracy. A crowding bias (measured in magnitudes) is applied by Reiss for individual Cepheids. Rarely a Cepheid will coincide almost exactly with a bright source causing it to be a significant outlier in the P–L relation, these are removed.

The photometric analysis between R11 and R16 is very similar, the main difference is that they do not list the bias corrections in the R16 data. In R16 they use a colour cut to eliminate outliers, since the major contaminants in the H-band are blending with a nearby red supergiant. However, because R11 and R16 do not list all of the Cepheids we can only match a small subset, meaning we do not know the bias correction of outliers excluded from the R16 fits.

R11 provides 165 Cepheids, 47 of which are excluded for the fits. R16 provides 139 Cepheids.

Figure 6 contains a comparison of both sets, including excluded points in R11, plotted against the R16 single fit calculated in (21). We can then calculate a residual for points vs the fit, Δm, to draw easier comparisons, plotted in figure 7.

We can run a single fit on the R11 Cepheids to see if fit parameters differ from R16. We find fitting for all 165 Cepheids including outliers:

$$\begin{aligned} 165 \text{ Cepheids} \quad & b = -2.927 \pm 0.062, \\ \text{All Periods} \quad & c = -6.067 \pm 0.038. \end{aligned} \tag{31a}$$

Now excluding the Reiss designated outliers:

$$\begin{aligned} 118 \text{ Cepheids} \quad & b = -3.131 \pm 0.109, \\ \text{All Periods} \quad & c = -6.012 \pm 0.051. \end{aligned} \tag{31b}$$

We see this fit does not differ very much from (29).

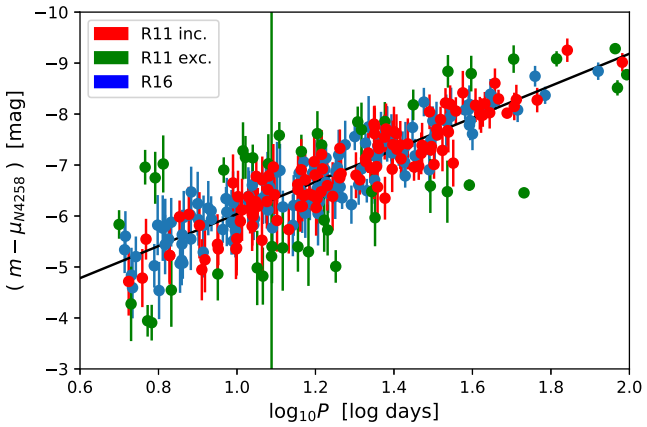

FIG. 6: Comparison of R16 and R11 data shown with excluded R11 Cepheids plotted against R16 fit (21)

From figure 7 it is clear there are significant outliers from the R11 fit, unaccounted for by the stated magnitude uncertainty. Four possibilities are given to explain these:

- Cepheid is near to a bright star (usually a red supergiant, though occasionally a blue supergiant).
- A poor model reconstruction of a crowded scene for a Cepheid.
- Misidentifation of a non-classical Cepheid.
- Cepheids are assigned the wrong period.

Figure 7 is alarming because the excluded (green) Cepheids are asymmetric and the negative green points have smaller errors than the positive green points. This at least raises the possibility that the R16 exclusion criteria may be biased.

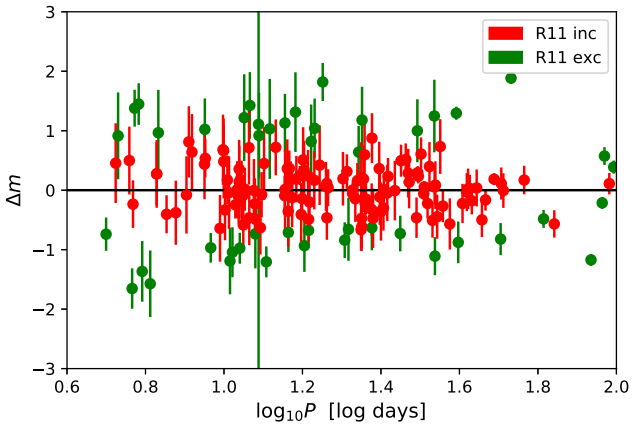

FIG. 7: Plot of R11 Cepheid residuals.

8.1 INVESTIGATION/PCA

We wish to see if we can explicitly identify any affirmation of a possible bias in R11 data. Identifying $(\Delta m, bias, P, color)$ for each Cepheid, we plot all combinations of variables against each other in figure 8.

No obvious trends appear. The bias does not seem to correlate significantly with Cepheid colour. Cepheids are bluer than the common source of light blending, red giants, so we'd expect redder Cepheids to require a bigger bias correction.

To investigate further we perform principle component analysis. The idea of this is to reduce the dimensionality of the data set, whilst retaining as much as possible of the variation present. We transform to a new set of variables, the principal components (PCs), which are uncorrelated, and ordered the first few retain most of the original variation present. It should show us concisely if any well defined relations exist.

First we normalise the data to account for scale differences. Dividing $(\Delta m, bias, P, color)$ by component standard deviation we define the basis:

$$(\hat{\Delta m} \ , \ \hat{bias} \ , \ \hat{P} \ , \ \hat{color} \ ). \tag{32}$$

Calculating associated covariance matrix:

$$X = \begin{pmatrix} 1 & 0.1969 & 0.0005 & -0.0284 \\ 0.1969 & 1 & -0.1235 & -0.1687 \\ 0.0005 & -0.1235 & 1 & 0.3618 \\ -0.0284 & -0.1687 & 0.3618 & 1 \end{pmatrix}. \tag{33}$$

There is some evidence for weak correlations between parameters looking at $Cov(P, color)$ and $Cov(\Delta m, bias)$. In figure 8 we can see Cepheids with the largest residuals have little crowd correction. This is somewhat surprising. Diagonalising the covariance matrix X we find eigenvalues and associated eigenvectors:

$$1.48, \begin{pmatrix} 0.227 \\ 0.748 \\ 0.624 \\ 0.002 \end{pmatrix}, \qquad 1.11, \begin{pmatrix} 0.464 \\ 0.476 \\ -0.740 \\ 0.103 \end{pmatrix},$$

$$0.77, \begin{pmatrix} -0.589 \\ 0.369 \\ -0.226 \\ -0.682 \end{pmatrix}, \qquad 0.63, \begin{pmatrix} -0.622 \\ 0.279 \\ -0.110 \\ 0.724 \end{pmatrix}. \tag{34}$$

The eigenvalues are of similar magnitude. We can't draw any conclusions about a linear relation between the four variables. The first eigenvector with largest eigenvalue has some resemblance of a Bias-Colour quality.

The PCA analysis shows that there are no obvious correlations of parameters with outliers.

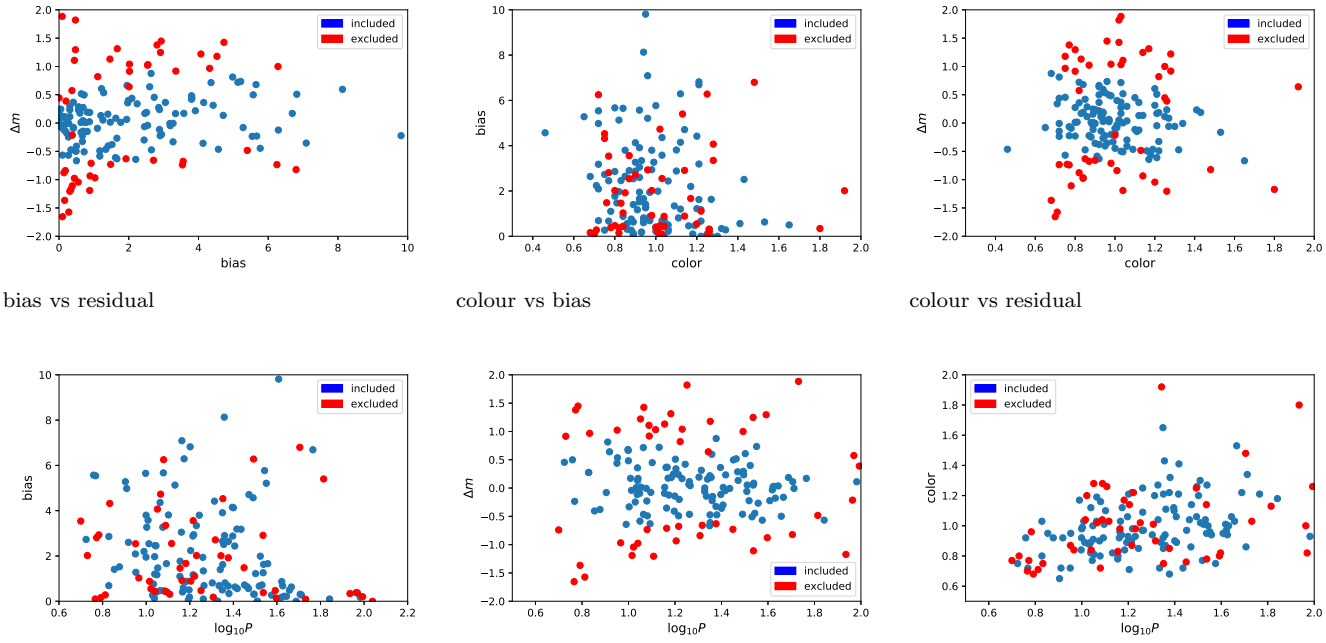

bias vs residual | colour vs bias | colour vs residual

period vs bias | period vs residual | period vs colour

FIG. 8: All combinations of $(\Delta m, bias, P, color)$ from R11 NGC 4258 data plotted against each other.

	Supernova			Cepheids			
Host	SN	$m_{0,v}$	$\sigma_{0,i}$	no.	no. $P < 10$ days	$< \sigma >$	Fitted μ_i from (41)
N4536	1981B	11.613	0.124	33		0.268	30.928 ± 0.059
N4639	1990N	12.419	0.115	25		0.360	31.593 ± 0.072
N3370	1994ae	12.912	0.116	63		0.333	32.097 ± 0.057
N3982	1998aq	12.231	0.115	16		0.301	31.703 ± 0.071
N3021	1995al	12.963	0.117	18		0.417	32.436 ± 0.083
N1309	2002fk	13.192	0.117	44		0.354	32.517 ± 0.062
N5584	2007af	12.701	0.116	83		0.325	31.801 ± 0.055
N4038	2007sr	12.233	0.115	13		0.428	31.387 ± 0.093
M101	2011fe	9.747	0.117	252	41	0.284	29.223 ± 0.051
N1015	2009ig	13.451	0.124	14		0.321	32.545 ± 0.080
N1365	2012fr	11.918	0.125	32		0.324	31.324 ± 0.064
N1448	2001el	12.201	0.116	54		0.302	31.352 ± 0.054
N2442	2015F	12.276	0.142	141		0.519	31.555 ± 0.059
N3447	2012ht	12.701	0.124	80		0.278	31.938 ± 0.052
N3972	2011by	12.484	0.116	42		0.492	31.659 ± 0.072
N5917	2005cf	13.008	0.115	13		0.393	32.288 ± 0.089
N7250	2013dy	12.303	0.116	22		0.445	31.539 ± 0.077
U9391	2003du	13.470	0.115	28		0.340	32.902 ± 0.067
N4424	2012cg	11.546	0.109	3		0.563	30.862 ± 0.012

TABLE II: Details for 19 SNe 1a host galaxies, number of Cepheids and fitted (41) distance moduli.

9 MEASURING THE HUBBLE CONSTANT

Now we determine H_0. To do this we perform a single, simultaneous fit to all Cepheid and SN Ia data to minimize the χ^2 statistic and measure the parameters of the distance ladder. We have 19 SNe 1a host galaxies to use from the SH0ES program. The program selected 1a SNe with the following qualities:

- Modern photometric data (photoelectric or CCD).
- SNe observed before maximum brightness and well after.
- Low reddening coefficient.
- A strong likelihood of being able to detect Cepheids in the host galaxy with HST.

In table 2 the SNe host galaxy details with B-band peak apparent magnitude $m_{0,v}$ and associated error are displayed. We express, as in R16, the jth Cepheid Magnitude in the ith host as:

$$(m_j^i)^e = (\mu_i - \mu_{N4258}) + c + b\log_{10} P_j^i + Z\Delta\log_{10}(O/H)_j^i. \quad (35)$$

where c now represents the apparent magnitude of a $\Delta\log_{10}(O/H) = 0$, $P = 1$ Cepheid in NGC 4258.

For convenience, we define a parameter $m^v_{0,N4258}$ which is the expected reddening-free peak magnitude of a SN Ia appearing in NGC 4258. We then express $m^v_{0,i}$, the peak apparent SN 1a magnitude at the time of B-band peak, in the ith host galaxy as:

$$(m^v_{0,i})^e = (\mu_i - \mu_{N4258}) + m^v_{0,N4258}. \quad (36)$$

We minimise for the combined χ^2 of:

$$\chi^2 = \sum_{i,j} \frac{(m_j^i - (m_j^i)^e)^2}{(\sigma_j^i)^2} + \sum_i \frac{(m^v_{0,i} - (m^v_{0,i})^e)^2}{(\sigma_{0,i})^2}, \quad (37)$$

to fit for parameters :

$$(\mu_1, ..., \mu_{19}, c, Z, b, m^v_{0,N4258}), \quad (38)$$

where $\sigma_{0,i}$ is the error associated with SN magnitude $m^v_{0,i}$.

R9 presents detailed calculation (Section 3) of the Hubble constant using fit parameters (38). H_0 is determined as:

$$\log_{10} H_0 = \frac{(m^v_{0,N4258} - \mu_{N4258}) + 5a_x + 25}{5}, \quad (39)$$

where μ_{N4258} is the independent, geometric distance estimate to NGC 4258 as in (18). The term a_x is the intercept of the SN Ia magnitude-redshift relation, measured from a set of SN Ia independent of any absolute (i.e. luminosity or distance) scale. This is determined from the Pantheon sample of over 600 SNe Ia (Scolnic et al. 2015) and used by R16 as:

$$a_x = 0.71273 \pm 0.00176. \quad (40)$$

The full statistical error in H_0 is the quadrature sum of the uncertainty in the three independent terms in equation (39): μ_{N4258} , $m^v_{0,N4258}$ and $5a_x$.

9.1 RESULTS

Fitting for restricted period range as described in section 7 we find:

$$\begin{aligned} &\text{no priors} & b &= -3.064 \pm 0.046, \\ &P > 10 \text{ days} & Z &= -0.168 \pm 0.075, \\ & & m^v_{0,N4258} &= 10.118 \pm 0.043, \\ & & H_0 &= 71.9 \pm 1.9 \text{km s}^{-1} \text{ Mpc}^{-1}. \end{aligned} \quad (41)$$

The fitted distance moduli for the 19 SN 1a host galaxies are included in Table 2 and the slopes are plotted in figure 9. We want to see how changing the slope affects the value of H_0. Using the LMC HST fit (17) slope value $b = -3.321$ as a prior input with a certainty of $\sigma_d = 0.001$ as in (12) we find:

$$\begin{aligned} &\text{(17) slope prior} & b &= -3.321 \pm 0.001, \\ &P > 10 \text{ days} & Z &= -0.159 \pm 0.075, \\ & & m^v_{0,N4258} &= 10.063 \pm 0.042, \\ & & H_0 &= 70.1 \pm 1.8 \text{km s}^{-1} \text{ Mpc}^{-1}. \end{aligned} \quad (42)$$

We see this brings H_0 closer to the Planck value (2). Investigating non-linearity in (30) we found an even steeper slope for LMC Cepheids $P > 10$ days. Using $b = -3.390$ as a prior input with a certainty of $\sigma_d = 0.001$ we find

$$\begin{aligned} &\text{(30) slope prior} & b &= -3.390 \pm 0.001, \\ &P > 10 \text{ days} & Z &= -0.157 \pm 0.075, \\ & & m^v_{0,N4258} &= 10.048 \pm 0.042, \\ & & H_0 &= 69.7 \pm 1.8 \text{km s}^{-1} \text{ Mpc}^{-1}. \end{aligned} \quad (43)$$

This is even closer to the Planck value. It seems if we use LMC slope constraints we can reduce the discrepancy. However, if we try the original no priors calculation (41) with the joint fit calculated NGC 4258 geometric distance (24) of $\mu^P_{NGC} = 29.221 \pm 0.029$ we find:

$$\begin{aligned} &\text{no priors} & b &= -3.064 \pm 0.046, \\ &P > 10 \text{ days} & Z &= -0.168 \pm 0.075, \\ &\mu^P_{NGC} \text{ as in (24)} & m^v_{0,N4258} &= 10.118 \pm 0.043, \\ & & H_0 &= 78.0 \pm 1.9 \text{km s}^{-1} \text{ Mpc}^{-1}. \end{aligned} \quad (44)$$

If the maser geometric distance to NGC 4258 (18) is wrong like the joint fit (24) might suggest, the H_0 discrepancy with Planck increases significantly.

We want to see what happens to the H_0 if we use LMC as a distance anchor instead of NGC 4258. If we swap LMC with NGC 4258 for the global fit analysis in section 9 and use the DEBs LMC geometric distance (13) we find:

$$\begin{aligned} &\text{no priors} & b &= -3.356 \pm 0.017, \\ &P > 10 \text{ days} & Z &= -0.175 \pm 0.077, \\ & & m^v_{0,LMC} &= -0.738 \pm 0.077, \\ & & H_0 &= 74.1 \pm 2.4 \text{km s}^{-1} \text{ Mpc}^{-1}. \end{aligned} \quad (45)$$

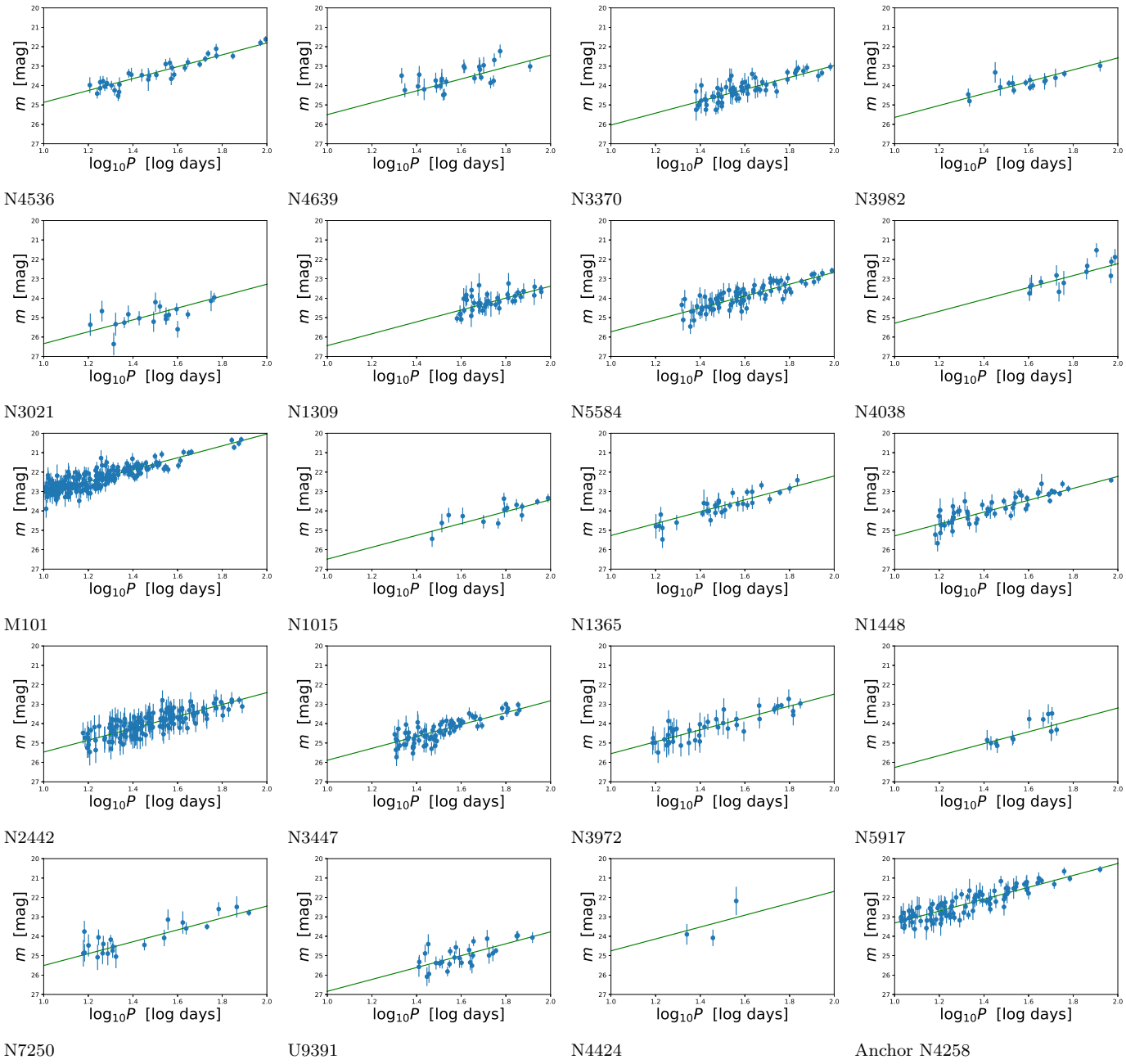

FIG. 9: Global fit (41) plotted for 19 SN 1a host galaxies and distance anchor NGC 4258.

10 CONCLUSION

We draw two main conclusions:

1. Geometric distance discrepancy between LMC and NGC 4258 distance anchors.

2. Discrepancy in the P-L relation slope between LMC, NGC 4258 and other SN 1a host galaxies.

We find a 3.5σ geometric distance moduli discrepancy in the distance anchors whilst performing a joint fit. This suggests either that calculations of the independent distance anchor moduli are incorrect or that Reiss's Cepheid photometry is biased.

There is also a significant slope discrepancy between the LMC $b = -3.390 \pm 0.060$ (30) and NGC plus SN host galaxies used in the global fit $b = -3.064 \pm 0.046$ of 4.3σ. Shallow slopes point to the potential of some systematic error or bias in Reiss's Cepheid photometry, particularly at large distances. Enforcing a steeper slope like we see in the LMC reduces the Planck/Distance ladder H_0 discrepancy significantly (43).

If the LMC distance anchor is correct, the H_0 tension actually increases (45). If the Cepheid photometry is biased, and we have a slope as indicated by $P > 10$ LMC Cepheids of $b = -3.390$ then H_0 decreases and there might be no significant tension with the Planck value at all.

11 FURTHER WORK

If further work was carried out, it would be useful to include the other two distance anchors used in R16, namely M31 and Milky Way Cepheids, running the global fit with these to see how they affect H_0 and which of the two distance anchors we used they are closer to agreement with.

We could also construct Monte-Carlo models to more carefully analyse the impact that certain photometry biases could have on the P-L slope and the resulting H_0 calculation.

12 REFERENCES

Freedman W. L., et al., 2012, ApJ, 758, 24
Knox L., Millea M., 2019, arXiv:1908.03663
Ngeow C.-C., Kanbur S. M., 2005, MNRAS, 360, 1033
Persson S. E., et al., 2004, AJ, 128, 2239
Pietrzynski G., Graczyk, D., Gallenne, A., et al., 2019, Nature, 567, 200
Planck Collaboration, 2018, arXiv:1807.06209
Reid M. J., Pesce D. W., Riess A. G., 2019, arXiv: 1908.05625
Reiss A. G., et al., 2009, arXiv: 0905.0695
Reiss A. G., et al., 2011, arXiv: 1103.2976
Reiss A. G., et al., 2016, arXiv: 1604.01424
Reiss A. G., et al., 2019, arXiv: 1903.07603
Scolnic D., Casertano S., Riess A., et al., 2015, ApJ, 815, 117
Scowcroft V., et al., 2011, arXiv:1108.4672